

Volcanic forcing improves Atmosphere-Ocean Coupled General Circulation Model scaling performance

Dmitry Vyushin,^{1,*} Igor Zhidkov,^{1,†} Shlomo Havlin,^{1,‡} Armin Bunde,^{2,§} and Stephen Brenner^{3,¶}

¹*Minerva Center and Department of Physics, Bar-Ilan University, Ramat-Gan 52900, Israel*

²*Institut für Theoretische Physik III, Justus-Liebig-Universität Giessen,
Heinrich-Buff-Ring 16, 35392 Giessen, Germany*

³*Department of Geography, Bar-Ilan University, Ramat-Gan 52900, Israel*

(Dated: November 15, 2018)

Recent Atmosphere-Ocean Coupled General Circulation Model (AOGCM) simulations of the twentieth century climate, which account for anthropogenic and natural forcings, make it possible to study the origin of long-term temperature correlations found in the observed records. We study ensemble experiments performed with the NCAR PCM for 10 different historical scenarios, including *no forcings*, *greenhouse gas*, *sulfate aerosol*, *ozone*, *solar*, *volcanic forcing* and various combinations, such as *natural*, *anthropogenic* and *all forcings*. We compare the scaling exponents characterizing the long-term correlations of the observed and simulated model data for 16 representative land stations and 16 sites in the Atlantic Ocean for these scenarios. We find that inclusion of volcanic forcing in the AOGCM considerably improves the PCM scaling behavior. The scenarios containing volcanic forcing are able to reproduce quite well the observed scaling exponents for the land with exponents around 0.65 independent of the station distance from the ocean. For the Atlantic Ocean, scenarios with the volcanic forcing slightly underestimate the observed persistence exhibiting an average exponent 0.74 instead of 0.85 for reconstructed data.

PACS numbers: 92.60.Wc, 92.70.Gt, 02.70.Hm, 92.60.Bh

While many modelers and climatologists focus their studies on trends caused by natural and anthropogenic forcings during the twentieth century [1, 2, 3, 4, 5, 6] we here focus on another important aspect of temperature anomalies - long-term correlations. One of the first studies on the question how general circulation models reproduce observed climate variability was performed by [7]. Using power spectrum analysis, which is affected by nonstationarities in time series, they argue that the GFDL AOGCM reproduced the natural climate variability on decadal and centennial scales correctly for a 1000 year control run integration. Several recent studies of [8, 9, 10, 11, 12, 13, 14] clearly demonstrate that surface air temperature (SAT) anomalies are long-term correlated with a fluctuation exponent α close to 0.65. On the other hand, results of [15, 16, 17, 18, 19] indicate that AOGCMs underestimate surface air temperature (SAT) persistence for control run, greenhouse gas forcing only and greenhouse gas forcing plus sulfate aerosols scenarios. In contrast, recent studies of reconstructed data [20, 21] claim that inner continental regions do not show long-term correlations, and thus AOGCMs successfully reproduce the natural persistence for the control run and greenhouse gas forcing only scenarios. Recently, this claim was tested on observed records by [22] with the finding that the SAT fluctuation exponents for continen-

tal sites do show long-term correlation and the α values do not depend on the distance of the site from the ocean.

In this Letter we show that the recent PCM model simulations properly reproduce the observed long-term correlations for SAT on land only for those scenarios that include volcanic forcing. These scenarios also show better scaling performance over the ocean than the other scenarios.

In order to present the land-surface temperature profile for the last century, 16 observed daily maximum temperature time series are considered. They have been collected from different representative weather stations around the globe for the following sites: Vancouver, Tucson, Cheyenne, Luling, Brookings, Albany, Oxford, Prague, Kasan, Tashkent, Surgut, Chita, Seoul, Yakutsk, Melbourne and Sydney. We also analyze the gridded monthly mean sea surface temperature (SST) for 16 sites in the Atlantic ocean with a spatial resolution of $2.5^\circ \times 2.5^\circ$ for the period of 1900 – 2002 from the Kaplan Extended SSTA data set (see also [23]). For 1900 – 1981 this is the analysis of [24] which uses optimal estimation in the space of 80 empirical orthogonal functions (EOFs) in order to interpolate ship observations of the U.K. Meteorological Office database [25]. The data after 1981 consists of gridded data from the National Center for Environmental Prediction optimal interpolation analysis, which combines ship observations with remotely sensed data [26]. This analysis is performed on the same set of 80 EOFs as used in [24] in order to provide enhanced data quality.

The model considered in our study is the Parallel Climate Model (PCM), which was developed at the National Center for Atmospheric Research (NCAR). It is a

*Electronic address: vjushin@ory.ph.biu.ac.il

†Electronic address: zhidkov@shoshi.ph.biu.ac.il

‡Electronic address: havlin@ophir.ph.biu.ac.il

§Electronic address: Armin.Bunde@theo.physik.uni-giessen.de

¶Electronic address: sbrenner@mail.biu.ac.il

fully coupled global ocean-atmosphere-sea ice-land surface model that produces a stable climate without flux adjustment. The horizontal resolution of the atmosphere is equivalent to $2.8^\circ \times 2.8^\circ$, with 18 levels in the vertical. Resolution of the ocean is roughly $2/3^\circ$, increasing to $1/2^\circ$ at the equator, with 32 levels. The detailed description of the model and results from experiments using various forcings and their combinations may be found in [3, 27, 28] and [4].

Here we study 10 forcing combinations: *no forcings*, *greenhouse gas*, *sulfate aerosol*, *ozone*, *solar*, *volcanic*, *solar + volcanic*, *ozone + solar + volcanic*, *greenhouse gas + sulfate aerosol + ozone*, *all forcings*. Greenhouse gas forcing is based on historical observations of CO_2 , N_2O , CH_4 , CFC-11, CFC-12, and ozone [28]. Evolution of direct forcing from tropospheric sulfate aerosol is reported by [29]. Historical changes of solar irradiance were reconstructed by [30] and volcanic forcing by [4]. The period of all experiments is 1890-1999.

For the no forcings and solar+volcanic scenarios we analyze the available 3-member ensembles, whereas for other scenarios 4-member ensembles are available. For each scenario, we selected the temperature records of the 4 grid points closest to each site, and bilinearly interpolated the data to the location of the observed site.

For each record, we analyse daily (or monthly) temperature anomalies ΔT_i . The ΔT_i are called long-term correlated if their autocorrelation function $C(s)$ decays with time lag s by a power law

$$C(s) \sim s^{-\gamma}, \quad 0 < \gamma < 1. \quad (1)$$

To overcome possible nonstationarities in the data, we do not calculate $C(s)$ directly. Instead we construct the ‘‘profile’’ $Y_n = \sum_{i=1}^n \Delta T_i$ and study the fluctuation function $F(s)$ of the profile in segments of length s by using the second order detrended fluctuation analysis (DFA2) [31, 32]. In DFA2 we determine in each segment the best second-order polynomial fit of the profile. The standard deviation of the profile from these polynomials represents the square of the fluctuations in each segment.

The fluctuation function $F(s)$ is the root mean square of the fluctuations in all segments. For the relevant case of long-term power-law correlations given by Eq. (1), with $0 < \gamma < 1$, the fluctuation function $F(s)$ increases according to a power law,

$$F(s) \sim s^\alpha, \quad \alpha = 1 - \frac{\gamma}{2}. \quad (2)$$

For uncorrelated data (as well as for short-range correlations represented by $\gamma \geq 1$ or exponentially decaying correlation functions), we have $\alpha = \frac{1}{2}$. For long-term correlations we have $\alpha > \frac{1}{2}$.

First we plot the results of DFA2 (DFA curves of higher order show the same performance) for the observed daily maximum temperature (Figure 1a) and NCAR PCM simulations from the B06.61 run (Figure 1b). Run B06.61 represents one of the runs from the all forcings ensemble.

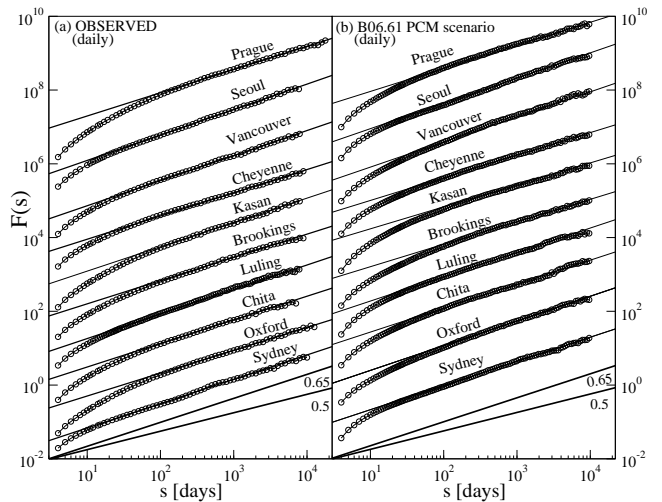


FIG. 1: DFA2 fluctuation functions $F(s)$ for the daily surface air maximum temperature anomalies at 10 land sites: (a) observed data and (b) NCAR PCM B06.61 (all forcings) simulated data. The scale of $F(s)$ is arbitrary. The straight lines crossing each curve represent the best asymptotic fit. The two lines shown at the bottom have slopes 0.65 and 0.5.

All curves are shown in a double logarithmic presentation. We plot 10 typical DFA curves chosen from our 16 sites over land. The sites chosen include coastal, near coastal, and inland locations.

The approximate period of the observed records is 1880-1990, with the maximum length for Prague (1775-1992) and the minimum for Seoul (1908-1993). The period of the B06.61 run is 1890-1999. The slopes in Figure 1a correspond to fluctuation exponents of the observed SAT anomalies, and vary from 0.62 to 0.68, with an average close to 0.65. Figure 1a demonstrates that SAT anomalies for all sites studied obey long-term power-law correlations independent of the distance from the nearest ocean. The slopes in Figure 1b range from 0.62 to 0.69. Comparing Figures 1a and 1b shows that the scaling of the NCAR PCM output agrees quite well with the scaling of the observed data over land.

Figure 2 shows DFA2 curves for the 10 sites in the Atlantic ocean for the Kaplan reconstructed monthly SST anomalies (Figure 2a) and for the NCAR PCM monthly averaged SST anomalies from the all forcings B06.61 run (Figure 2b). The slopes for the reconstructed SSTA vary from 0.71 in the equatorial part of the Atlantic to 1.0 in the Northern Atlantic, with an average of 0.85. The SSTA exponents characterizing the memory effect on decadal and centennial scales seem to depend on complex ocean circulation dynamics. The variation of the scaling exponents over the Atlantic Ocean is significantly larger than on land, which is probably due to different ocean circulation patterns in equatorial, mid-latitude, and high-latitude regions. In a double logarithmic presentation, the slopes of the DFA2 curves for the simulated ocean records have an average of 0.72 which is noticeably lower

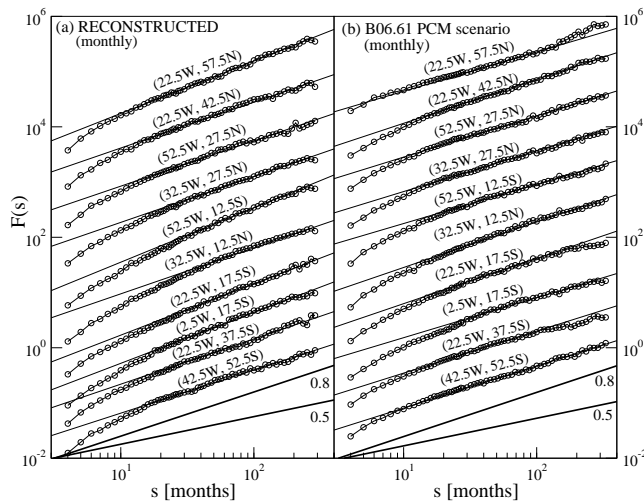


FIG. 2: DFA2 fluctuation functions $F(s)$ for monthly sea surface temperature anomalies at 10 sites in the Atlantic ocean : (a) the Kaplan reconstructed data and (b) NCAR PCM B06.61 (all forcings) run. The scale of $F(s)$ is arbitrary. The straight lines crossing each curve represent the best asymptotic fit. The two lines shown at the bottom have slopes 0.8 and 0.5.

than the observed average of 0.85.

Figure 3 presents the fluctuation exponent distribution for the observed data and for the 10 NCAR PCM scenarios considered for the 16 land locations. In each panel the “grey” column in the range $[0.62, 0.68]$ represents the distribution of the fluctuation exponents for the observed data. As seen from the figure, scenarios containing volcanic forcing best reproduce the observations since they have a peak at the same range $[0.62-0.68]$ as the observed data. Their average fluctuation exponent is close to 0.65. In contrast, the other six scenarios that do not contain volcanic forcing, have an average fluctuation exponent for land less than 0.6 (see also [17]).

Similar behavior is found over the Atlantic Ocean. Only those scenarios containing the volcanic forcing exhibit an average fluctuation exponent greater than 0.7 with the largest value equal to 0.76 for the volcanic forcing only scenario. Figure 4 shows the fluctuation exponent distribution for the Atlantic Ocean for the Kaplan data (in grey) and for 10 studied scenarios (in black). Thus the PCM underestimates the fluctuation exponents obtained for reconstructed data for the Atlantic Ocean by 10-15%.

Therefore, we can conclude that for the NCAR PCM addition of volcanic forcing to any other forcing combination immediately improves its scaling behavior both for the land and the ocean. This fact suggests that (besides the atmosphere-ocean coupling) the volcanic forcing is mostly responsible for the presence of the long-term correlations in the NCAR PCM over land on annual and decadal scales. For the ocean, the addition of volcanic forcing leads to stronger memory and consequently higher fluctuation exponents comparing to those for the

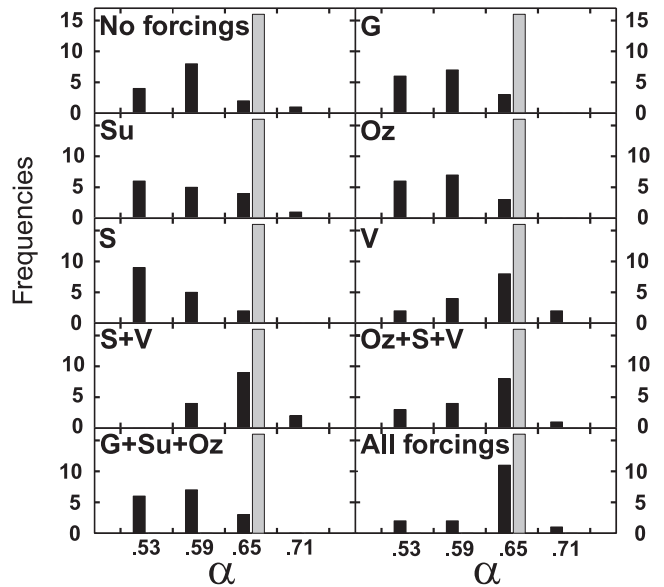


FIG. 3: Histograms of the fluctuation exponents α for the observed records (grey column) and the simulated records, for land stations. The considered 10 scenarios are: no forcings, greenhouse gas (G), sulfate (Su), ozone (Oz), solar (S), volcanic (V), solar + volcanic (S+V), ozone + solar + volcanic (Oz+S+V), greenhouse gas + sulfate + ozone (G+Su+Oz), and all forcings. Four bins in each panel correspond to α in the intervals $[0.5, 0.56)$, $[0.56, 0.62)$, $[0.62, 0.68)$, and $[0.68, 0.74]$ respectively. The grey column in each panel corresponds to the fluctuation exponent distribution for the observed records, the black columns are for simulated records.

land. However the NCAR PCM still underestimates the observed persistence of the oceans.

The main conclusion from our research is that the NCAR PCM is able to reproduce the scaling behavior of the observed land SAT records for the last century after taking into account all historically based natural and anthropogenic forcings. However, even the best scenario for the land slightly underestimates natural SST persistence in the ocean, possibly due to errors in the simulations of deep ocean circulation, the atmosphere-ocean interaction, and/or an insufficiently long spin up period of the ocean component of the AOGCM.

The results presented in this letter may also help to clarify the controversy about the values of SAT fluctuation exponents for inner continental regions (see [20]). Our study indicates that not only the observed records for inner continental regions are long-term correlated in agreement with [22], but also the recent PCM simulations for these regions show similar fluctuation exponents, characteristic of long-term persistence.

Finally, this letter also supports the suggestion of [17] that the inability of the seven leading AOGCMs, for their control runs, greenhouse gas forcing only, and greenhouse gas plus aerosols scenarios, to mimic the observed SAT persistence is caused by the absence of natural forcings, in particular volcanic forcing. The results of our detrended

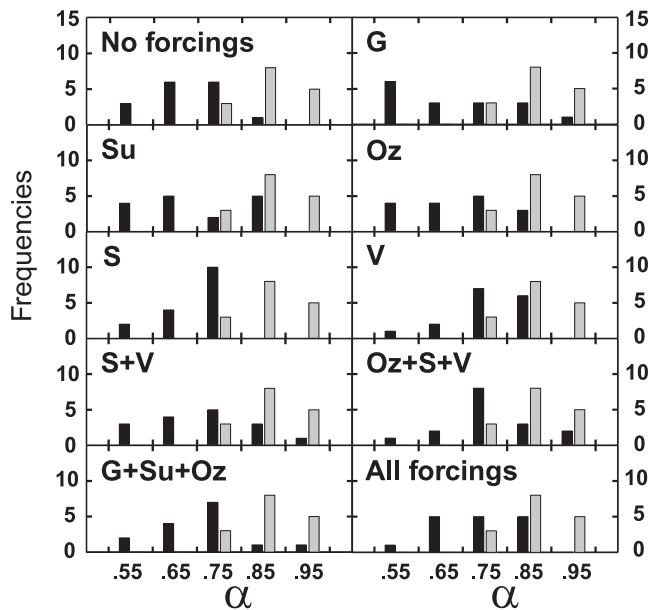


FIG. 4: Histograms for the fluctuation exponents for the reconstructed (in grey) and simulated (in black) records for the Atlantic Ocean. The five bins correspond to α values in the intervals $[0.5,0.6)$, $[0.6,0.7)$, $[0.7,0.8)$, $[0.8,0.9)$, and $[0.9,1.0]$ respectively.

fluctuation analysis for the 16 land stations around the globe and the 16 sites in the Atlantic ocean suggest that volcanic forcing has by far the largest impact on the AOGCM long-memory persistence.

Acknowledgments

This work has been supported by the Deutsche Forschungsgemeinschaft and the Israel Science Foundation. We are grateful to W. M. Washington, M. Wehner, and G. Strand for providing access to the NCAR PCM simulations data. The authors thank J. Eichner, J. Kantelhardt and E. Koscielny-Bunde for fruitful discussions.

-
- [1] Stott, P. A., S. F. B. Tett, G. S. Jones, M. R. Allen, J. F. B. Mitchell, G. J. Jenkins, External control of 20th century temperature by natural and antropogenic forcings, *Science*, **290**, 2133 (2000).
 - [2] Mitchell, J. F. B., et al., Detection of Climate change and Attribution of Causes, in *Climate Change 2001: The scientific Basis Contribution of Working Group I to the Third Assessment Report of the Intergovernmental Panel on Climate Change*[Houghton, J. T. et al., Eds], *Cambridge University Press* (2001).
 - [3] Meehl, G.A., W. M. Washington, T. M. L. Wigley, J. M. Arblaster, A. Dai, Solar and greenhouse gas forcing and climate response in the twentieth century, *J. Clim.*, **16**, 426 (2003).
 - [4] Ammann, C. M., G. A. Meehl, W. M. Washington and C. S. Zender, A monthly and latitudinally varying volcanic forcing dataset in simulations of 20th century climate, *Geophys. Res. Lett.*, **30**, 1657 (2003).
 - [5] Santer, B. D., et al., Contributions of Antropogenic and Natural Forcing to Recent Tropopause Height Changes, *Science*, **301** (2003).
 - [6] von Storch, H., and G. Floeser (Eds.), *Anthropogenic Climate Change*, Springer Verlag; Berlin, Heidelberg (1999).
 - [7] Manabe, S., and R. Stouffer, Low-Frequency Variability of Surface Air Temperature in a 1000-Year Integration of a Coupled Atmosphere-Ocean-Land Surface Model, *J. Clim.*, **9**, 376 (1996).
 - [8] Koscielny-Bunde, E., A. Bunde, S. Havlin, Y. Goldreich, Analysis of daily temperature fluctuations, *Physica A*, **231**, 393 (1996).
 - [9] Koscielny-Bunde, E., A. Bunde, S. Havlin, H. E. Roman, Y. Goldreich, H. J. Schellnhuber, Indication of a universal persistence law governing atmospheric variability, *Phys. Rev. Lett.*, **81**, 729 (1998).
 - [10] Pelletier, J. D., and D. L. Turcotte, Long-range persistence in climatological and hydrological time series: analysis, modeling and application to drought hazard assessment, *J. Hydrol.*, **203**, 198 (1997).
 - [11] Talkner, P. and R. O. Weber, Power spectrum and detrended fluctuation analysis: Application to daily temperatures, *Phys. Rev. E*, **62**, 150 (2000).
 - [12] Pelletier, J. D., Natural variability of atmospheric temperatures and geomagnetic intensity over a wide range of time scales, *PNAS*, **99**, 2546 (2002).
 - [13] Caballero, R., S. Jewson, A. Brix, Long memory in surface air temperature: detection, modeling, and application to weather derivative valuation, *Climate Research*, **21(2)**, 127 (2002).
 - [14] Eichner, J. F., E. Koscielny-Bunde, A. Bunde, S. Havlin, H. J. Schellnhuber, Power-law persistence and trends in the atmosphere: a detailed study of long temperature records, *Phys. Rev. E*, **68**, 046133 (2003).
 - [15] Bell, J., P. Duffy, C. Covey and L. Sloan, Comparison of temperature variability in observations and sixteen climate model simulations, *Geophys. Res. Lett.*, **27**, 261 (2000).
 - [16] Govindan, R. B., D. Vyushin, S. Brenner, A. Bunde, S. Havlin, H. J. Schellnhuber, Long-range correlations and trends in global climate models: Comparison with real data, *Physica A*, **294**, 239 (2001).
 - [17] Govindan, R. B., D. Vyushin, A. Bunde, S. Brenner, S. Havlin, H.J. Schellnhuber, Global climate models violate scaling of the observed atmospheric variability, *Phys. Rev. Lett.*, **89**, 028501 (2002).

- [18] Syroka, J., and R. Toumi, Scaling and persistence in observed and modelled surface temperature, *Geophys. Res. Lett.*, **28**, 3255 (2001).
- [19] Vjushin, D., R. B. Govindan, S. Brenner, A. Bunde, S. Havlin, H. J. Schellnhuber, Lack of scaling in global climate models, *Journal of Physics: Condensed Matter*, **14**, 2275 (2002).
- [20] Fraedrich, K. and R. Blender, Scaling of Atmosphere and Ocean Temperature Correlations on Observations and Climate Models, *Phys. Rev. Lett.*, **90**, 108501 (2003).
- [21] Blender, R. and K. Fraedrich, Long Time Memory in Global Warming Simulations, *Geophys. Res. Letters*, **30**(14), 1769 (2003).
- [22] Bunde, A., J. F. Eichner, S. Havlin, E. Koscielny-Bunde, H. J. Schellnhuber and D. Vyushin, Comment on "Scaling of atmosphere and ocean temperature correlations in observations and climate models", E-print cond-mat/0305080, *Phys. Rev. Lett.*, **in press** (2004).
- [23] Monetti, R. A., S. Havlin, and A. Bunde, Long term persistence in the sea surface temperature fluctuations, *Physica A*, **320**, 581 (2003).
- [24] Kaplan, A., M. A. Cane, Y. Kushnir, A. C. Clement, M. B. Blumenthal, B. Rajagopalan, Analyses of global sea surface temperature 1856-1991, *J. of Geophys. Res.*, **103**, 18567 (1998).
- [25] Parker, D. E., P. D. Jones, C. K. Folland, A. Bevan, Interdecadal changes of surface temperature since the late nineteenth century, *J. of Geophys. Res.*, **99**, 14,373 (1994).
- [26] Reynolds, R. and T. Smith, Improved global sea-surface temperature analyses using optimum interpolation, *J. Climate*, **7**, 929 (1994).
- [27] Washington, W. M., et al., Parallel Climate Model (PCM) control and transient simulations, *Clim. Dynam.*, **16**, 755 (2000).
- [28] Dai, A., T. M. L. Wigley, B. A. Boville, J. T. Kiehl, L. E. Buja, Climates of the twentieth and twenty-first centuries simulated by the NCAR climate system model, *J. Clim.*, **14**, 485-519 (2001).
- [29] Kiehl, J. T., T. L. Schneider, P. J. Rasch, M. C. Barth, and J. Wong, Radiative forcing due to sulfate aerosols from simulations with the National Center for Atmospheric Research Community Climate Model, Version 3, *J. Geophys. Res.*, **105**(D1), 1441-1457 (2000).
- [30] Hoyt, D. V., and K. H. Schatten, A discussion of plausible solar irradiance variations, 1700-1992, *J. Geophys. Res.*, **98**(A11), 18,895-18,906 (1993).
- [31] Peng, C.-K., S. V. Buldyrev, S. Havlin, M. Simons, H. E. Stanley, A. L. Goldberger, On the mosaic organization of DNA nucleotides, *Phys. Rev. E*, **49**, 1685 (1994).
- [32] Kantelhardt, J. W., E. Koscielny-Bunde, H. H. A. Rego, S. Havlin, A. Bunde, Detecting long-range correlations with detrended fluctuation analysis, *Physica A*, **295**, 441 (2001).